



University of Bahrain  
**Journal of the Association of Arab Universities for  
Basic and Applied Sciences**

www.elsevier.com/locate/jaaubas  
www.sciencedirect.com



# Synthesis and spectral, antibacterial, molecular studies of biologically active organosilicon(IV) complexes



Har Lal Singh\*, J.B. Singh, Sunita Bhanuka

Department of Chemistry, College of Engineering and Technology, Mody University of Science and Technology, Lakshmanagarh 332311, India

Received 17 February 2016; revised 28 April 2016; accepted 17 May 2016  
Available online 11 June 2016

## KEYWORDS

Thiosemicarbazone;  
Semicarbazone;  
Organosilicon(IV) complexes;  
Spectroscopy;  
Antimicrobial activity;  
Density functional theory calculations

**Abstract** A series of new organosilicon(IV) complexes have general formulae  $R_3SiL$  and  $RSiLOEt$  with Schiff bases ( $R = Me$  and  $Ph$ ). The Schiff bases (LH) have been derived from the condensation of (2-hydroxyphenyl)(pyrrolidin-1-yl)methanone with semicarbazide, thiosemicarbazide, and phenylthiosemicarbazide, respectively. The compounds have been characterized by the elemental analysis, molar conductance, and spectral (UV, IR,  $^1H$ ,  $^{13}C$ , and  $^{29}Si$  NMR) studies. These studies showed that the ligands coordinate with the silicon atom in a tridentate manner through phenolic oxygen, azomethine nitrogen and thiolic sulfur. Further applying experimental spectroscopic techniques, theoretical data calculated using density functional theory by B3LYP/6.31 + g(d,p) has also been used for structural determination. The resulting complexes have been proposed to have trigonal bipyramidal and distorted octahedral geometries. Few representative Schiff base and their silicon complexes have been screened for their in vitro antibacterial activity against Gram-positive and Gram-negative bacteria. The minimum inhibitory concentration (MIC) of selected compounds was determined. The screening results show that organosilicon(IV) complexes have better antibacterial activity than the free ligands.

© 2016 University of Bahrain. Publishing services by Elsevier B.V. This is an open access article under the CC BY-NC-ND license (<http://creativecommons.org/licenses/by-nc-nd/4.0/>).

## 1. Introduction

The chemistry of complexes with hypercoordinated silicon atoms is attractive from many points of view such as reactivity, biological activity, and structural features as reported (Chuit et al., 1999; Devi et al., 2012) previously. Schiff base complex compounds have taken a wide place in coordination chemistry

and have an important role in the development of bioinorganic chemistry and biochemistry (Ali et al., 2012; Mohamed et al., 2014; Kothari and Sharma, 2014; Savithiri et al., 2014; Singh, 2009). Metal complexes of the Schiff bases possess numerous applications including antibacterial, antifungal and other biological applications, as well as clinical, analytical and industrial in addition to their important roles in catalysis. Thiosemicarbazones and semicarbazones compound possessing varied significant biological activity have been reported, such as antifungal (Nath et al., 2000; Thanh et al., 2015; Reis et al., 2013), antibacterial (Kalaivani et al., 2012; Singh et al., 2014), antitumor

\* Corresponding author.  
E-mail address: [hlsingh9@rediffmail.com](mailto:hlsingh9@rediffmail.com) (H.L. Singh).  
Peer review under responsibility of University of Bahrain.

(Tojal, 2012; Arora et al., 2014), anti-inflammatory (Asif and Husain, 2013), antileukemia (Pahontu et al., 2015), cytotoxic (Silva et al., 1998), antioxidant (Singhal et al., 2011), anticonvulsant (Kumar and Raj, 2013), and anticancer (Naidu and Kinthada, 2012; Kulandaivelu et al., 2011), activities. Metal complexes of the Schiff bases possess numerous applications including antibacterial, antifungal, antiviral, anticancer and other biological applications, as well as clinical, analytical and industrial in addition to their important roles in catalysis.

Keeping in view the biological and medicinal importance of thiosemicarbazones, semicarbazones and the role of metal ions in biology, we herein report the synthesis of a new series of Schiff bases from the condensation reaction of (2-hydroxyphenyl)(pyrrolidin-1-yl)methanone with semicarbazide, thiosemicarbazide, and phenylthiosemicarbazide. These synthesized Schiff bases were further used to react with organosilicon (IV) ions to form their respective organosilicon(IV) complexes with the hope that these compounds would form a novel class of silicon-based bioactive compounds and, moreover, may have a tendency to reduce the resistivity of bacterial strains. The synthesized ligands and their organosilicon(IV) complexes have been investigated for in vitro antibacterial activity against Gram-negative and two Gram-positive bacterial strains.

## 2. Experimental

### 2.1. Materials and methods

Adequate care was taken to keep the organosilicon(IV) complexes, chemicals, and glass apparatus free from moisture; clean and well-dried glass apparatus fitted with quick fit interchangeable standard ground joints was used throughout the experimental work. All reagents were purchased from Aldrich, Merck and were used as such. The solvents were dried and purified according to the standard method. Melting points were determined in an open glass capillaries and were uncorrected. The ligands were prepared by the condensation of (2-hydroxyphenyl)(pyrrolidin-1-yl)methanone with semicarbazide, thiosemicarbazide, and phenylthiosemicarbazide as described earlier (Singh et al., 2015, 2016).

### 2.2. Analytical methods

Silicon was determined gravimetrically as SiO<sub>2</sub>. Nitrogen and sulfur were estimated by Kjeldahl's and Mesenger's methods, respectively. Molecular weights were determined by the Rast camphor method. Infrared spectra were recorded on a Perkin Elmer, IR SP-2 spectrometer. <sup>1</sup>H, <sup>13</sup>C and <sup>29</sup>Si NMR spectra were recorded in DMSO-d<sub>6</sub> using tetramethylsilane as internal standard on a Bruker Avance II FTNMR 400 MHz spectrometer. UV-visible spectra were recorded on an Agilent Carry 60 UV-visible double-beam spectrophotometer at room temperature in DMSO. Systronics Conductivity Bridge (model 305) was used for molar conductance of the organosilicon(IV) complexes at room temperature.

### 2.3. Computational methods

In order to understand the molecular geometry optimization of the compounds were performed with the Gaussian 03 software package, and Gauss view visualization program (Frisch et al., 2004; Becke, 1986) using the B3LYP/6.31 + g(d,p) basic sets to

predict the molecular structures. Calculations were carried out with Becke's three parameter hybrid model using the Lee-Yang-Parr correlation functional (B3LYP) method.

### 2.4. Syntheses of trimethylsilicon(IV) complexes and phenylsilicon(IV) complexes

A weighed amount of trimethylethoxysilane and triethoxyphenylsilane in dry methanol was added to the calculated amount of the ligands in 1:1 M ratio. The contents were refluxed on a fractionating column for about 10–12 h and the ethanol liberated in the reaction was removed with solvent. Excess solvent was removed under reduced pressure and the compounds were dried under vacuum at 40 ± 5 °C after repeated washing with dry cyclohexane. The compounds were purified by recrystallization from the same solvent. The purity was further checked by TLC using silica gel G.

#### 2.4.1. Compound 1: Me<sub>3</sub>SiL<sup>1</sup> was prepared by trimethylethoxysilane with ligand (L<sup>1</sup>H)

Light Brown solid; yield, 65.9%; melting point, 164 °C and elemental analysis (%), calcd. For C<sub>15</sub>H<sub>24</sub>N<sub>4</sub>OSSi: Si, 8.35; C, 53.54; H, 7.19; N, 16.65; S, 9.53; found: Si, 8.27, C, 53.45; H, 7.10; N, 16.56; S, 9.44; molecular weight: found, 330.67, calcd. 336.67. Molar conductance (DMF, 10<sup>-3</sup>, ohm<sup>-1</sup> mol<sup>-1</sup> cm<sup>2</sup>): 13.8; Infrared (KBr, cm<sup>-1</sup>): ν(C=N), 1624; ν(C=O), 1265; ν(C-S), 856; ν(Si ← N), 498; ν(Si-O), 560; ν(Si-C), 717. UV-Vis (λ<sub>max</sub>, nm): 230, 290, 360; <sup>1</sup>H NMR (DMSO-d<sub>6</sub>, δ ppm, 400 MHz): 7.35–7.26 (m, 2H, aromatic), 7.50 (d, 1H, J = 7.2 Hz, aromatic) 6.98 (d, 1H, J = 8.0 Hz, aromatic), 3.46–3.18 and 1.88–1.78 (m, 8H, pyrrolidine); 3.90 (s, 2H, NH<sub>2</sub>); 1.08 (s, 9H, Si-Me). <sup>13</sup>C NMR (DMSO, δ ppm, 100 MHz): 169.1 (C-S), 143.8 (C=N), 45.6, 44.7 (—CH<sub>2</sub>—CH<sub>2</sub>—, pyrrolidine); 25.6, 24.9 (—CH<sub>2</sub>—CH<sub>2</sub>—, pyrrolidine); 133.3, 131.8, 129.1, 121.7, 120.8, 109.1 (aromatic carbons); 13.3 (Si-Me); <sup>29</sup>Si NMR (DMSO, δ ppm,): -110.10.

#### 2.4.2. Compound 2: Me<sub>3</sub>SiL<sup>2</sup> was prepared by trimethylethoxysilane with ligand (L<sup>2</sup>H)

White creamy solid; yield, 71.58%; melting point, 170 °C and elemental analysis (%), calcd. for C<sub>21</sub>H<sub>28</sub>N<sub>4</sub>OSSi: Si, 6.81; C, 61.13; H, 6.84; N, 13.58; S, 7.77; found: Si, 6.75, C, 61.03; H, 6.75; N, 13.58; S, 7.65; molecular weight: found, 410.46, calcd., 412.62. Molar conductance (DMF, 10<sup>-3</sup>, ohm<sup>-1</sup> mol<sup>-1</sup> cm<sup>2</sup>): 15.5; Infrared (KBr, cm<sup>-1</sup>): ν(C=N), 1622; ν(C=O) 1272; ν(C-S) 845; ν(Si ← N), 486; ν(Si-O), 556; ν(Si-C), 732. UV-Vis (λ<sub>max</sub>, nm): 230, 285, 375; <sup>1</sup>H NMR (DMSO-d<sub>6</sub>, δ ppm, 400 MHz): 7.56–7.25 (m, 7H, aromatic), 7.76 (d, 1H, J = 6.9 Hz, aromatic) 6.96 (d, 1H, J = 8.0 Hz, aromatic), 3.50–3.18 and 1.90–1.78 (m, 8H, pyrrolidine); 4.54 (s, 2H, NH-Ph); 1.12 (s, 9H, Si-Me). <sup>13</sup>C NMR (DMSO, δ ppm, 100 MHz): 168.4 (—C—S), 159.5 (C=N), 44.8, 44.1 (—CH<sub>2</sub>—CH<sub>2</sub>—, pyrrolidine); 24.7, 23.98 (—CH<sub>2</sub>—CH<sub>2</sub>—, pyrrolidine); 132.5, 130.8, 130.1, 128.1, 122.3, 119.2, 117.1, 116.6, 115.5 (aromatic carbons); 10.8 (Si-Me); <sup>29</sup>Si NMR (DMSO, δ ppm,): -107.71.

#### 2.4.3. Compound 3: Me<sub>3</sub>SiL<sup>3</sup> was prepared by trimethylethoxysilane with ligand (L<sup>3</sup>H)

Light gray powder; yield, 80.14%; melting point, 98 °C and elemental analysis (%), calcd. for C<sub>15</sub>H<sub>24</sub>N<sub>4</sub>O<sub>2</sub>Si: Si, 8.76; C, 56.22;

H, 7.55; N, 17.48; found: Si, 8.68, C, 55.10; H, 7.50; N, 17.35; molecular weight: found, 311.87, calcd., 4320.46. Molar conductance (DMF,  $10^{-3}$ ,  $\text{ohm}^{-1} \text{mol}^{-1} \text{cm}^2$ ): 10.6; Infrared (KBr,  $\text{cm}^{-1}$ ):  $\nu(\text{C}=\text{N})$ , 1635;  $\nu(\text{C}-\text{O})$  1265;  $\nu(\text{Si}-\text{N})$ , 478;  $\nu(\text{Si}-\text{O})$ , 582;  $\nu(\text{Si}-\text{C})$ , 716. UV-Vis ( $\lambda_{\text{max}}$ , nm): 226, 290, 364;  $^1\text{H}$  NMR (DMSO- $d_6$ ,  $\delta$  ppm, 400 MHz): 7.50–7.24 (m, 2H, aromatic), 7.62 (d, 1H,  $J = 6.8$  Hz, aromatic) 6.88 (d, 1H,  $J = 8.2$  Hz, aromatic), 3.52–3.18 and 1.90–1.86 (m, 8H, pyrrolidine); 3.74 (s, 2H,  $\text{NH}_2$ ); 1.09 (s, 9H, Si–Me).  $^{13}\text{C}$  NMR (DMSO,  $\delta$  ppm, 100 MHz): 168.9 (–C–O), 156.2 (C=N), 45.6, 44.7 (– $\text{CH}_2$ – $\text{CH}_2$ –, pyrrolidine); 24.9, 23.7 (– $\text{CH}_2$ – $\text{CH}_2$ –, pyrrolidine); 131.3, 127.6, 123.8, 121.3, and 116.7 (aromatic carbons); 9.11 (Si–Me);  $^{29}\text{Si}$  NMR (DMSO,  $\delta$  ppm.): –105.1.

#### 2.4.4. Compound 4: $\text{PhSi}(\text{L}^1)\text{OEt}$ was prepared by triethoxyphenylsilane with ligand ( $\text{L}^1\text{H}$ )

Light gray solid; yield, 84.6%; melting point, 120 °C and elemental analysis (%), calcd. for  $\text{C}_{20}\text{H}_{24}\text{N}_4\text{O}_2\text{SSi}$ : Si, 6.81; C, 58.22; H, 5.86; N, 13.58; S, 7.77; found: Si, 6.67; C, 58.10; H, 5.88; N, 13.46; S, 7.70; molecular weight: found, 401.66, calcd. 412.58. Molar conductance (DMF,  $10^{-3}$ ,  $\text{ohm}^{-1} \text{mol}^{-1} \text{cm}^2$ ): 11.2; Infrared (KBr,  $\text{cm}^{-1}$ ):  $\nu(\text{C}=\text{N})$ , 1625;  $\nu(\text{C}-\text{O})$  1274;  $\nu(\text{C}-\text{S})$  860;  $\nu(\text{Si}-\text{N})$ , 482;  $\nu(\text{Si}-\text{O})$ , 570. UV-Vis ( $\lambda_{\text{max}}$ , nm): 235, 280, 372;  $^1\text{H}$  NMR (DMSO- $d_6$ ,  $\delta$  ppm, 400 MHz): 7.48–7.16 (m, 2H, aromatic), 7.62 (d, 1H,  $J = 7.0$  Hz, aromatic) 6.94 (d, 1H,  $J = 8.0$  Hz, aromatic), 3.51–3.18 and 1.96–1.88 (m, 8H, pyrrolidine); 3.74 (s, 2H,  $\text{NH}_2$ ).  $^{13}\text{C}$  NMR (DMSO,  $\delta$  ppm, 100 MHz): 172.9 (–C–S), 161.7 (C=N), 45.7, 44.3 (– $\text{CH}_2$ – $\text{CH}_2$ –, pyrrolidine); 25.6, 24.9 (– $\text{CH}_2$ – $\text{CH}_2$ –, pyrrolidine); 131.6, 127.3, 123.4, 119.5, 115.8 (aromatic carbons);  $^{29}\text{Si}$  NMR (DMSO,  $\delta$  ppm.): –97.98.

#### 2.4.5. Compound 5: $\text{PhSi}(\text{L}^2)\text{OEt}$ was prepared by triethoxyphenylsilane with ligand ( $\text{L}^2\text{H}$ )

Gray solid; yield, 74.07%; melting point, 118 °C and elemental analysis (%), calcd. for  $\text{C}_{26}\text{H}_{28}\text{N}_4\text{O}_2\text{SSi}$ : Si, 5.75; C, 63.90; H, 5.78; N, 11.47; S, 6.56; found: Si, 5.70, C, 63.78; H, 5.84; N, 11.44; S, 6.50; molecular weight: found, 469.99, calcd., 488.68. Molar conductance (DMF,  $10^{-3}$ ,  $\text{ohm}^{-1} \text{mol}^{-1} \text{cm}^2$ ): 15.5; Infrared (KBr,  $\text{cm}^{-1}$ ):  $\nu(\text{C}=\text{N})$ , 1628;  $\nu(\text{C}-\text{O})$ , 1275;  $\nu(\text{C}-\text{S})$ , 850;  $\nu(\text{Si}-\text{N})$ , 470;  $\nu(\text{Si}-\text{O})$ , 585. UV-Vis ( $\lambda_{\text{max}}$ , nm): 220, 270, 368;  $^1\text{H}$  NMR (DMSO- $d_6$ ,  $\delta$  ppm, 400 MHz): 7.68–7.12 (m, 7H, aromatic), 7.78 (d, 1H,  $J = 6.9$  Hz, aromatic) 6.98 (d, 1H,  $J = 8.2$  Hz, aromatic), 3.51–3.12 and 1.92–1.85 (m, 8H, pyrrolidine); 4.52 (s, 2H,  $\text{NH}-\text{Ph}$ ).  $^{13}\text{C}$  NMR (DMSO,  $\delta$  ppm, 100 MHz): 167.9 (–C–S), 155.1 (C=N), 45.6, 44.6 (– $\text{CH}_2$ – $\text{CH}_2$ –, pyrrolidine); 25.6, 24.9 (– $\text{CH}_2$ – $\text{CH}_2$ –, pyrrolidine); 131.9, 130.5, 130.1, 127.6, 122.6, 118.4, 116.8, 116.1, 115.8 (aromatic carbons);  $^{29}\text{Si}$  NMR (DMSO,  $\delta$  ppm.): –92.34.

#### 2.4.6. Compound 6: $\text{PhSi}(\text{L}^3)\text{OEt}$ was prepared by triethoxyphenylsilane with ligand ( $\text{L}^3\text{H}$ )

White creamy solid; yield, 75.0%; melting point, 94 °C and elemental analysis (%), calcd. for  $\text{C}_{20}\text{H}_{24}\text{N}_4\text{O}_3\text{Si}$ : Si, 7.08; C, 60.58; H, 6.10; N, 14.13; found: Si, 7.0, C, 60.65; H, 6.02; N, 14.19; molecular weight: found, 390.88, calcd., 396.52. Molar conductance (DMF,  $10^{-3}$ ,  $\text{ohm}^{-1} \text{mol}^{-1} \text{cm}^2$ ): 14.7; Infrared (KBr,  $\text{cm}^{-1}$ ):  $\nu(\text{C}=\text{N})$ , 1630;  $\nu(\text{C}-\text{O})$  1268;  $\nu(\text{Si}-\text{N})$ , 465;  $\nu(\text{Si}-\text{O})$ , 560. UV-Vis ( $\lambda_{\text{max}}$ , nm): 225, 290, 370.  $^1\text{H}$  NMR (DMSO- $d_6$ ,  $\delta$  ppm, 400 MHz): 7.50–7.10 (m, 2H, aromatic), 7.60 (d, 1H,

$J = 6.8$  Hz, aromatic) 6.85 (d, 1H,  $J = 8.0$  Hz, aromatic), 3.50–3.18 and 1.90–1.78 (m, 8H, pyrrolidine); 3.66 (s, 2H,  $\text{NH}_2$ ).  $^{13}\text{C}$  NMR (DMSO,  $\delta$  ppm, 100 MHz): 168.2 (–C–O), 160.64 (C=N), 45.6, 44.7 (– $\text{CH}_2$ – $\text{CH}_2$ –, pyrrolidine); 23.9, 23.8 (– $\text{CH}_2$ – $\text{CH}_2$ –, pyrrolidine); 131.0, 128.3, 123.1, 121.4, 116.5 (aromatic carbons);  $^{29}\text{Si}$  NMR (DMSO,  $\delta$  ppm.): –95.85.

### 2.5. Biological assay

#### 2.5.1. In vitro antibacterial screening

Fresh cultures of standard bacteria viz. *Bacillus cereus* (MTCC 430), *Escherichia coli* (MTCC 443), *Klebsiella pneumoniae* (MTCC 109) and *Staphylococcus aureus* (MTCC 3381) were collected from microbiology lab. Synthesized compounds were screened for their antibacterial activity against *B. cereus*, *E. coli*, *K. pneumoniae* and *S. aureus* at a concentration of 200 ppm by the agar well diffusion method (Singh et al., 2014). 5 ml aliquot of nutrient broth was inoculated with the test organisms and incubated at 35 °C for 24 h. Sterile nutrient agar plates were also prepared and holes of 6 mm diameter were cut using a sterile cork borer ensuring proper distribution. The test organisms after 24 h of incubation were spread onto separate agar plates. The chemical compounds dissolved in DMSO were poured into appropriately labeled holes using a pipette in aseptic conditions. A hole containing DMSO served as a negative control. Triplicate plate of each bacterial strain was prepared. The plates were incubated aerobically at 35 °C for 24 h. The antimicrobial activity was determined by measuring the diameter of the zone (mm) showing complete inhibition with respect to control (DMSO).

#### 2.5.2. Determination of minimum inhibitory concentration (MIC)

MIC was determined by serial dilution method. Drugs and compounds with inhibitory zones against the above mentioned bacterial strains were used in this part. The two fold serial dilution technique (Al-Burtamani et al., 2005) was used to determine minimum inhibitory concentration (MIC) values. In this method, the various test concentrations of synthesized compounds were made from 200 to 0.39  $\mu\text{g}/\text{ml}$  in sterile tubes No. 1–10. 100  $\mu\text{L}$  sterile Nutrient Broth was poured in each sterile tube followed by addition of 200  $\mu\text{L}$  test compound in tube 1. Two fold serial dilutions were carried out from tube No. 1 to tube 10. The incubating period for the bacteria was 24 h at 35 °C. The lowest concentration of a compound that resulted in complete inhibition of the visible microbial growth after incubation was recorded as the MIC value. Streptomycin and Ciprofloxacin were taken as standard bactericide, for assessing the activity results.

## 3. Results and discussion

### 3.1. Chemistry

Schiff base derivatives (LH) of semicarbazone and thiosemicarbazones were prepared by the condensation reaction of (2-hydroxyphenyl)(pyrrolidin-1-yl)methanone with semicarbazide, thiosemicarbazide and phenylthiosemicarbazide. All the synthesized Schiff base derivatives are soluble in methanol, DMF and DMSO at room temperature. The organosilicon(IV) complexes prepared from these ligands were obtained by the reaction of the corresponding ligands with the silicon(IV) ions in a 1:1 M ratio (Scheme 1). They are moderately soluble in

common organic solvents and completely soluble in DMF and DMSO. Their physical properties and analysis are recorded in Section 2.

### 3.2. Conductance measurements

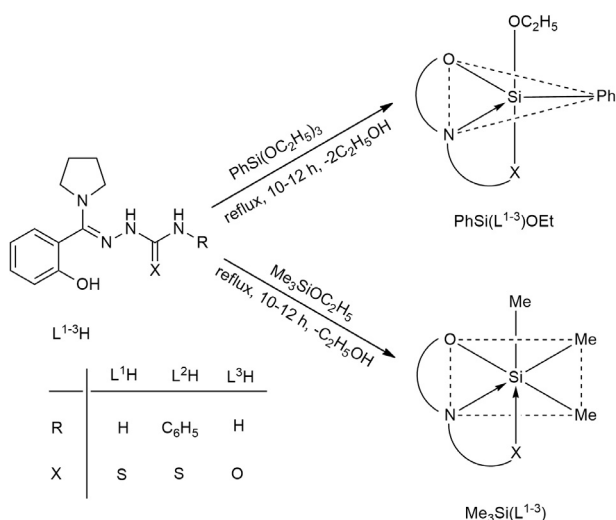
The molar conductance of all the organosilicon(IV) complexes (1–6) was observed at room temperature in DMF as a solvent and their results in ( $\Omega^{-1} \text{ cm}^2 \text{ mol}^{-1}$ ) are recorded. The molar conductance values of all the organosilicon(IV) complexes at room temperature fall in the range 10.9–15.7  $\Omega^{-1} \text{ cm}^2 \text{ mol}^{-1}$ , indicating that these complexes are non-electrolytic in nature.

### 3.3. Spectroscopic characterization

#### 3.3.1. IR spectra

The characteristic bands in the IR spectra data of organosilicon (IV) complexes are reported in Section 2. The infrared spectra of complexes are given in [Supplementary material \(Figs. S1–S6\)](#). The disappearance of original bands at 3325 and 1715  $\text{cm}^{-1}$  due to amino ( $\text{NH}_2$ ) and keto ( $>\text{C}=\text{O}$ ) groups and, in turn, the appearance of a new band at 1613–1625  $\text{cm}^{-1}$  assigned to the azomethine ( $-\text{C}=\text{N}$ ) linkage ([Singh et al., 2001](#)) provided a clue to the condensation of amine with ketone resulting in the formation of the desired Schiff bases. All the Schiff base ligands possessed potential donor sites such as the phenolic oxygen ( $\text{Ph}-\text{O}$ ), azomethine nitrogen ( $-\text{C}=\text{N}$ ), and thiolic sulfur ( $-\text{C}-\text{S}$ ), which have a tendency to coordinate with the silicon ions. The IR spectra of all the ligands exhibited absorption bands at 1613–1625, 1282–1295, 875–945, 1380 and 1695  $\text{cm}^{-1}$ , respectively, assigned to the vibrations  $\nu(\text{C}=\text{N})$ ,  $\nu(\text{C}-\text{O})$ ,  $\nu(\text{N}-\text{N})$ ,  $\nu(\text{C}=\text{S})$  and  $\nu(\text{C}=\text{O})$ . Comparison of the IR spectra of the Schiff base ligands with corresponding silicon complexes provided further evidence of the coordination of the silicon ions with the Schiff base ligands. The overall conclusions may be drawn from the comparison:

1. All the Schiff base ligands showing IR bands at 1613–1625  $\text{cm}^{-1}$  due to azomethine nitrogen shifted ([Singh et al., 2012, 2013a,b,c](#)) to a lower frequency (10–18  $\text{cm}^{-1}$ )



**Scheme 1** Synthesis of organosilicon(IV) complexes.

at 1622–1635  $\text{cm}^{-1}$ , representing involvement of the azomethine nitrogen in coordination with the silicon atom.

2. In the spectra of ligands a strong band at  $\sim 3300 \text{ cm}^{-1}$  that corresponds to the  $\nu(\text{OH})$  group have disappeared in the spectra of complexes due to the deprotonation, indicating coordination through the phenolic oxygen to silicon(IV) atom.
3. The free ligands showed a band at  $\sim 1290 \text{ cm}^{-1}$  which is due to  $\nu(\text{C}-\text{O})$ . This band is shifted to lower wave numbers at  $1265 \pm 10 \text{ cm}^{-1}$  in the organosilicon(IV) complexes, indicating the coordination of phenolic oxygen to the organosilicon(IV) atom. This coordination was supported by the appearance ([Singh and Singh, 2000](#)) of a new band at 445–460  $\text{cm}^{-1}$  assigned to  $\nu(\text{Si}-\text{O})$ .
4. The IR spectra of the ligands show medium intensity bands in the regions of  $\sim 3105 \text{ cm}^{-1}$  and  $\sim 2748 \text{ cm}^{-1}$  which may be assigned to  $\nu(\text{N}-\text{H})$  and  $\nu(\text{S}-\text{H})$  vibrations, respectively. Other bands in the region of 1343–1330  $\text{cm}^{-1}$  due to  $\nu(\text{C}=\text{S})$  suggest that ligands exist in the thiol-thione tautomerism. These bands disappeared in the spectra of silicon (IV) complexes and a new band appeared in the range 870–848  $\text{cm}^{-1}$  which was assigned to  $\nu(\text{C}-\text{S})$  ([Wang et al., 2013](#)). This indicates the deprotonation of the thiol group, which supports chelating through sulfur atom.
5. In all the organosilicon(IV) complexes, a new band appearing at 520–532  $\text{cm}^{-1}$  due to  $\nu(\text{Si}-\text{N})$  vibrations indicated the coordination of azomethine nitrogen with the silicon atom ([Kadish et al., 1988](#)).
6. In trimethyl and phenyl silicon complexes, the bands at 1422, 1120, 715 and 700  $\text{cm}^{-1}$  have been attributed to the asymmetric and symmetric modes of  $\text{Si}-\text{CH}_3$  and  $\text{Si}-\text{C}_6\text{H}_5$  groups ([Malhotra et al., 2007](#)), which do not appear in the spectra of ligands.
7. The bands observed at 3445 and 3370  $\text{cm}^{-1}$  are due to the symmetric and asymmetric modes of amino ( $\text{NH}_2$ ) group. These bands are observed at almost the same position in the spectra of organosilicon complexes suggesting the non-involvement of this amino group in coordination. All other bands remain unchanged in the spectra of all ligands and their corresponding silicon complexes.

The IR spectra of all ligands and their organosilicon(IV) complexes conclusively showed that the ligands acted as tridentate and coordinated with the silicon atoms via the azomethine nitrogen, phenolic oxygen, and thiolic-sulfur/ketonic-oxygen atoms.

#### 3.3.2. <sup>1</sup>H NMR spectra

The <sup>1</sup>H NMR spectral data of organosilicon(IV) complexes are reported in Section 2. <sup>1</sup>H NMR spectra of complexes are given in [Supplementary material \(Figs. S7 and S8\)](#). The exhibited signals of all the protons due to aromatic groups were found to be in their expected region. The <sup>1</sup>H NMR spectra of free ligands showed resonance signals at  $\sim \delta$  12.90, 9.05, 7.75–6.74, and 3.54–1.92, ppm, due to OH, NH, aromatic protons, and pyrrolidine protons, respectively. The <sup>1</sup>H NMR spectra of the ligands exhibit, peaks at  $\sim \delta$  12.90(s) and 9.05 (s) ppm characteristic of the  $-\text{OH}$  and  $-\text{NH}$  protons, respectively. After complexation, the disappearance of the signal due to  $-\text{OH}$  and  $\text{NH}$  protons in the spectra of silicon complexes indicates the deprotonation of these groups and that supports the coordination of ligand through oxygen atom to the central silicon atom. Further, the appearance of signals due to  $\text{NH}_2$  protons at the same positions

in the ligands and their complexes, confirms the non-participation of this group in coordination. The ligands give a complex multiplet signal in the region of  $\delta$  7.75–6.85 ppm for the aromatic protons, and these remain at almost the same position in the spectra of the silicon complexes. The new signals at  $\sim\delta$  1.75 ppm and  $\sim\delta$  6.20 ppm in trimethyl and phenylsilicon (IV) complexes are due to  $\text{Me}_3\text{Si}$  and  $\text{PhSi}$  groups, respectively.

### 3.3.3. $^{13}\text{C}$ NMR spectra

The  $^{13}\text{C}$  NMR spectral data of ligands and their silicon complexes were recorded in DMSO and reported in Section 2.  $^{13}\text{C}$  NMR spectra of complexes are given in [Supplementary material \(Figs. S9–S11\)](#). The proposed coordination in these complexes has been supported by the shifting in chemical shift values of the carbon atoms attached to the azomethine nitrogen atom, phenolic oxygen atom and thiolic sulfur atom. The signals due to the carbon atom attached to the azomethine group in the ligands appear at  $\delta$  166.2  $\pm$  1.70 ppm. However, in the spectra of the corresponding silicon complexes, these appear at  $\delta$  158.4  $\pm$  2.2 ppm. The considerable shift in the resonance of the carbon atom attached to nitrogen indicates that the azomethine nitrogen has been involved in coordination. The signals due to the carbon atoms attached to the  $\text{C}=\text{S}/\text{C}=\text{O}$  groups in ligands appear at  $\delta$  181.5–179.4 ppm. In the spectra of the corresponding silicon complexes, these signals appear at  $\delta$  172.6–168.4 ppm. The considerable shifts in the positions of these signals clearly indicate the involvement of these functional groups in bond formation with the silicon atom. The carbon of methyl groups ( $\text{Si}-\text{CH}_3$ ) is observed at a position comparable to other similar compounds. A signal due to carbon of ethyl group attached to silicon appeared at  $\sim$ 17.8 ppm, while the carbon atom of the phenyl group attached to the silicon moiety appeared at 146.9–135.9 ppm. Signals due to aromatic carbon atoms of the ligands appeared in the range 131.9–115.3 ppm, which remain almost same in the spectra of silicon complexes. The conclusions drawn from these studies provided further support to the modes of bonding already explained in the IR and  $^1\text{H}$  NMR spectral data.

### 3.3.4. $^{29}\text{Si}$ NMR spectra

In order to confirm the geometry of the complexes,  $^{29}\text{Si}$  NMR spectra of the complexes was recorded. The value of  $\delta$   $^{29}\text{Si}$  in the spectra reflects the coordination number of the nucleus in the corresponding silicon complexes ([Sedaghat and Pour, 2009](#); [Singh et al., 2013a,b,c](#); [Mohamed et al., 2006](#)).  $^{29}\text{Si}$  NMR spectra of silicon complexes give a sharp signal at  $\sim\delta$  –92.7 ppm and  $\delta$  –107.2 ppm which are in good agreement with the values for penta- and hexa-coordinated state around the silicon atoms. The spectra show in each case only one sharp singlet indicating the formation of a single species and  $^{29}\text{Si}$  H NMR spectrum of  $\text{Me}_3\text{SiL}^2$  (2) is given in [Fig. 1](#). On the basis of above spectral studies, the following five and six coordinated geometries have been suggested for  $\text{PhSi(L)OEt}$  and  $\text{Me}_3\text{SiL}$  types of complexes, respectively.

### 3.3.5. Electronic spectra

The mode of bonding and the geometry of these complexes were established with the help of different spectral studies. The electronic spectra of ligands and their organosilicon(IV) complexes were measured in dry methanol. The electronic spectra of ligands exhibit maxima at  $\sim$ 380 nm, which could

be assigned to the  $n-\pi^*$  transition of the azomethine group which undergoes a lower side in the silicon(IV) complexes due to the polarization within the  $>\text{C}=\text{N}$  chromospheres group caused by the silicon–ligand interaction. This clearly indicates the coordination of azomethine nitrogen atom to the silicon atom ([Varshney et al., 2000](#)). Ligands exhibit another two bands at around  $\sim$ 225 nm and  $\sim$ 276 nm, due to  $\pi-\pi^*$  transitions, which may be due to the  $\pi-\pi^*$  transition of benzenoid and  $\pi-\pi^*$  transition of  $\text{C}-\text{OH}$ , chromospheres, respectively. These bands remain approximately at same positions or minor change in the spectra of the silicon complexes.

## 3.4. Theoretical calculations

### 3.4.1. Structure optimization

Several attempts to grow appropriate crystal for X-ray crystallography were unsuccessful. The optimized parameters (bond lengths and bond angles) of Schiff base  $\text{L}^3\text{H}$  and  $\text{Me}_3\text{SiL}^3$  and  $\text{PhSiL}^3\text{OEt}$  obtained using the B3LYP/6-311++G(d,p) basic sets are listed in [Tables 1 and 2](#). The optimized structures of  $\text{Me}_3\text{SiL}^3$  and  $\text{PhSiL}^3\text{OEt}$  are shown in [Figs. 2 and 3](#). The most important bonds of the Schiff base compounds are  $\text{C}=\text{N}$ ,  $\text{Ph}-\text{OH}$  and  $\text{C}=\text{O}$  groups. These bond lengths of  $\text{L}^3\text{H}$  were calculated as 1.2685, 1.3732 and 1.2033 Å, respectively. On the other hand, these  $\text{C}=\text{N}$ ,  $\text{Ph}-\text{OH}$  and  $\text{C}=\text{O}$  bond lengths were obtained as 1.2794/1.2788, 1.4444/1.4479 and 1.2733/1.2754 Å in the organosilicon(IV) complexes. These results show that  $\text{C}=\text{N}$  bonds of the ligand weaken upon complexation. In addition, the carbonyl bond length was calculated as 1.2733 and 1.2754 Å in the  $\text{Me}_3\text{SiL}^3$  and  $\text{PhSiL}^3\text{OEt}$  complexes. The deprotonated ligand is coordinated as tridentate ligand *via* the ketonic oxygen, azomethine nitrogen and phenolic oxygen atoms. The organic molecule acts as tridentate with the ONO donors atoms. Since the synthesized compounds are related and differ only in substituted groups,

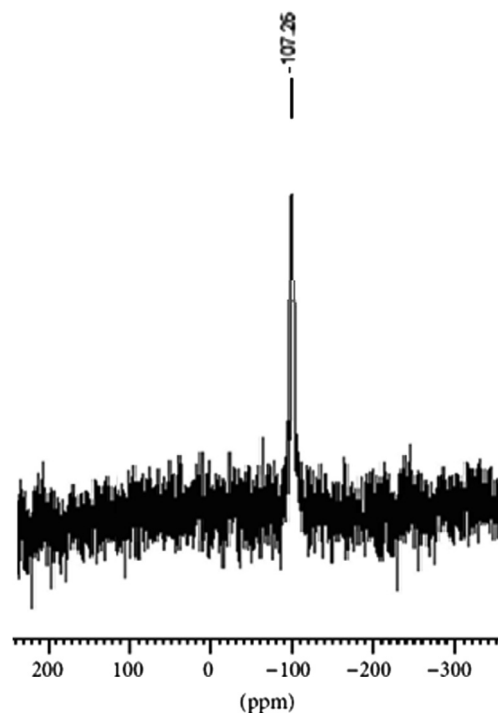


**Figure 1**  $^{29}\text{Si}$  NMR Spectrum of  $\text{Me}_3\text{SiL}^2$  complex.

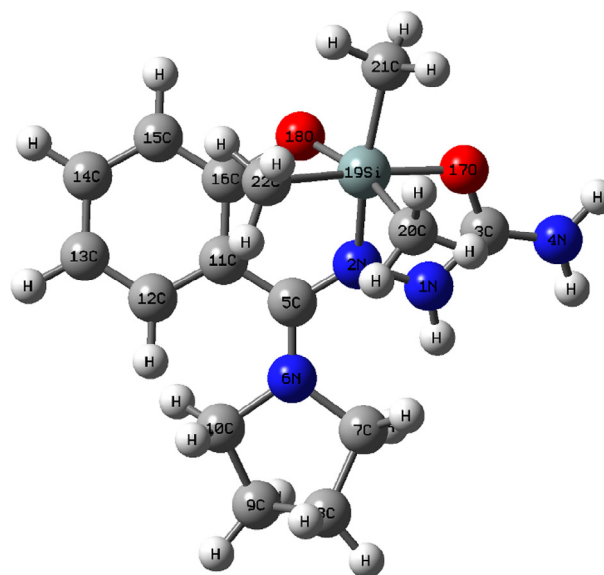
**Table 1** Selected bond lengths (Å) of  $L^3H$ ,  $Me_3SiL^3$  and  $PhSiL^3OEt$  compounds.

Atom connectivity	Bond length (Å)		
	$L^3H$	$Me_3SiL^3$	$PhSiL^3OEt$
C(5)—N(2)	1.2685	1.2794	1.2788
C(16)—O(18)	1.3732	1.4444	1.4479
O(17)—C(3)	1.2033	1.2733	1.2754
Si(19)—N(2)	—	1.8545	1.8114
Si(19)—O(17)	—	1.8492	1.8227
Si(19)—O(18)	—	1.6579	1.5811
Si(19)—C(20)	—	1.9400	1.9399
Si(19)—C(21)	—	1.9400	—
Si(19)—C(22)	—	1.9400	—
Si(19)—O(21)	—	—	1.6654

two compounds were theoretically studied. In compound (3) the value of the Si—N distance, is 1.8545 Å and Si—O in the range 1.8492/1.6579 Å, and in compound (6) the value of the Si—N distance, is 1.8114 Å and Si—O in the range 1.8227/1.5811 Å, which are similar to the already reported by X-ray structures of  $MeSi\{[OC_6H_3(OMe)C(Ph)N]_2(CH_2)_2\}(NCS)$ , complexes (González-García et al., 2009). The calculated Si—N bond distance is also close to that already reported by the X-ray crystal study of silicon(IV) complexes ( $Si\{[OC_6H_3(OMe)C(Ph)N]_2(CH_2)_2\}(NCS)_2$  and  $SiO_4$  N skeletons) (González-García et al., 2009; Seiler et al., 2007). In compound (3) bond angles C(20)—Si(19)—O(18) angle of 96.26°, O(18)—Si(19)—O(17) angle of 90.41°, C(22)—Si(19)—O(18) angle of 177.42°, C(20)—Si(19)—O(17) angle of 173.13° and C(21)—Si(19)—N(2) angle of 160.81° are in good agreement with the values reported for six coordinated silicon complexes (González-García et al., 2009). For the compound (6) optimized values of bond angles C(21)—Si(19)—N(2) angle of 114.02°, O(20)—Si(19)—C(21) angle of 131.18°, O(18)—Si(19)—O(17) angle of 167.93° and O(20)—Si(19)—O(18) angle of 97.63° are in good agreement with the values reported for five coordinated silicon complexes (Seiler et al., 2007).

### 3.4.2. Frontier molecular orbitals

The HOMOs and LUMOs are known as Frontier molecular orbitals, which played an important role for evaluating molecular chemical stability, chemical reactivity, chemical hardness

**Figure 2** Optimized structure of  $Me_3Si(L^3)$ .

and chemical softness of the molecule (Tang et al., 2011). The HOMO and LUMO energy, energy gap ( $\Delta E$ ), chemical potential ( $\mu$ ), electronegativity ( $\chi$ ), chemical hardness ( $\eta$ ), global softness ( $S$ ), electrophilicity index ( $\omega$ ) and dipole moment of  $L^3H$ ,  $Me_3SiL^3$  and  $PhSiL^3OEt$  are listed in Table 3. In the HOMO and LUMO analysis, the figure shows orbital density plots of HOMO and LUMO for the ligand, in which the LUMO surface mostly is delocalized on the aromatic ring. In the surface shown for the HOMO level, the C=N group is overlapped. In this molecular system, Figs. S12–S14 shows that the 3D plots of the HOMO frontier orbital density is located around the silicon atom; meanwhile, the density of the LUMO frontier orbital is in the ligand and tends to move toward the functional groups. As depicted in Table 3,  $L^3H$  has a larger energy gap than its silicon complexes. The energy gap,  $\Delta E$ , is directly involved in the chemical hardness/softness of a chemical species. Furthermore, the chemical hardness of a system implies resistance to charge transfer, whereas global softness is proportional to the polarizability of the system. Another electrophilicity index ( $\omega$ ) describes the electron

**Table 2** Selected bond angles (°) of  $Me_3SiL^3$  and  $PhSiL^3OEt$  complexes.

Atom connectivity	Bond angles (°)	Atom connectivity	Bond angles (°)
<i>Me<sub>3</sub>SiL<sup>3</sup> (compound 3)</i>			
C(20)—Si(19)—C(21)	90.8083	C(21)—Si(19)—N(2)	160.8128
C(20)—Si(19)—C(22)	84.2452	C(22)—Si(19)—O(18)	177.4195
C(20)—Si(19)—O(18)	96.2605	C(22)—Si(19)—O(17)	89.017
C(20)—Si(19)—O(17)	173.1277	C(22)—Si(19)—N(2)	99.8385
C(20)—Si(19)—N(2)	106.2661	O(18)—Si(19)—O(17)	90.411
C(21)—Si(19)—C(22)	90.3503	O(18)—Si(19)—N(2)	82.4627
C(21)—Si(19)—O(18)	87.1137	O(17)—Si(19)—N(2)	76.1837
C(21)—Si(19)—O(17)	87.8742		
<i>PhSiL<sup>3</sup>OEt (Compound 6)</i>			
O(20)—Si(19)—C(21)	131.1873	C(21)—Si(19)—O(17)	86.0797
O(20)—Si(19)—O(18)	97.6322	C(21)—Si(19)—N(2)	114.0176
O(20)—Si(19)—O(17)	93.6157	O(18)—Si(19)—O(17)	167.9339
O(20)—Si(19)—N(2)	113.6939	O(18)—Si(19)—N(2)	92.8357
C(21)—Si(19)—O(18)	89.7716	O(17)—Si(19)—N(2)	78.5856

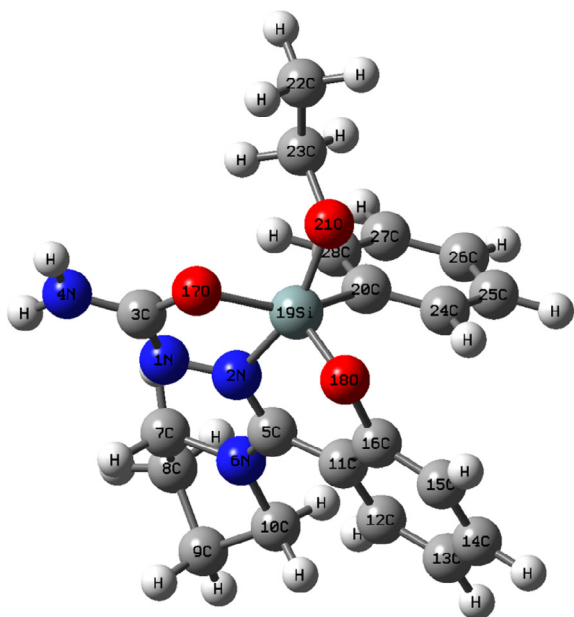


**Figure 3** Optimized structure of  $\text{PhSi}(\text{L}^3)\text{OEt}$ .

accepting ability of the systems. High values of the electrophilicity index increase the electron accepting abilities of the molecules. Thus, the electron accepting abilities of LH and their complexes are arranged in the following order:  $\text{Me}_3\text{SiL}^3 > \text{PhSiL}^3\text{OEt} > \text{L}^3\text{H}$ .

### 3.4.3. Mulliken atomic charges

The Mulliken atomic charges of  $\text{L}^3\text{H}$ ,  $\text{Me}_3\text{SiL}^3$  and  $\text{PhSiL}^3\text{OEt}$  compounds are calculated by B3LYP/6-31++G(d,p) and hf/6-31++G(d,p) basic sets. The Mulliken atomic charge calculation has an important role in the application of quantum chemical calculation to molecular system because atomic charges affect dipole moment, molecular polarizability, electronic structure, and a lot of properties of molecular system (Sidir et al., 2010). The results are shown in Tables S1–S3. The Mulliken charge distribution of ligand shows that the carbonyl oxygen atom is more negative (−0.574) as compared to phenolic oxygen and azomethine nitrogen atoms (−0.418 and −0.065). The lower negative charges on nitrogen atoms are

**Table 3** Calculated energy parameters of ligand ( $\text{L}^3\text{H}$ ) and their  $\text{Me}_3\text{SiL}^3$ ,  $\text{PhSiL}^3\text{OEt}$  complexes by B3LYP/6-31++g(d,p).

Property	Compounds		
	$\text{L}^3\text{H}$	$\text{Me}_3\text{SiL}^3$	$\text{PhSiL}^3\text{OEt}$
SCF energy (a.u.)	−836.316	−1244.864	−1510.732
$E_{\text{HOMO}}$ (eV)	−5.111	−3.772	−3.324
$E_{\text{LUMO}}$ (eV)	−0.571	−1.435	−0.756
Energy gap ( $\Delta E$ , eV)	4.540	2.337	2.568
Electronic chemical potential ( $\mu$ )	−2.841	−2.604	−2.040
Electronegativity ( $\chi$ )	2.841	2.604	2.040
Chemical hardness ( $\eta$ )	4.540	2.337	2.568
Global softness (S)	0.2203	0.4279	0.3894
Electrophilicity index ( $\omega$ )	0.8889	1.4508	0.8103
Dipole moment (Debye)	8.2429	14.0375	7.6195

due to the charge transfer in O—H/N-type intra-molecular hydrogen bonds. On the other hand, in the silicon(IV) complex, the charges of the all O and N atoms are negative, except the N atoms of amino groups. However, these negative charges are lower than the observed in ligand. The charge of the  $\text{Si}^{4+}$  ion in the Free State is +4.0. It is seen that the positive charge of the silicon ion decreases to 2.4046 in  $\text{Me}_3\text{SiL}^3$  complex and 2.641 in  $\text{PhSiL}^3\text{OEt}$ , which indicates that transfer of electrons from the ligand to the silicon ion has occurred and the coordination bonds have formed. The silicon(IV) atom has a positive charge in complexes. It has been noted that all hydrogen atoms are positively charged. It has also been observed that some carbon atoms are positive and some are negative. In ligand ( $\text{L}^3\text{H}$ ), C3, C5, C11, C14 and C15 are positively charged atoms, while the remaining is negatively charged. In the complex ( $\text{Me}_3\text{SiL}^3$ ), C3, C5, C7 and C11 are positively charged atoms, while the others are negatively charged. In the complex ( $\text{PhSiL}^3\text{OEt}$ ), C3, C6, C7, C11, C12 and C15 are positively charged atoms, while the remaining is negatively charged. Such a type of charge distribution generates the total dipole moment of 8.2429, 14.0375 and 7.6195 Debye for  $\text{L}^3\text{H}$ ,  $\text{Me}_3\text{SiL}^3$  and  $\text{PhSiL}^3\text{OEt}$ , respectively.

### 3.5. Antibacterial activity

The ligands ( $\text{L}^1\text{H}$  and  $\text{L}^3\text{H}$ ), silicon complexes, standard drugs and DMSO were screened for their antibacterial activity against Gram-negative bacteria (*E. coli* (MTCC 0443), *K. pneumoniae* (MTCC 0109)) and Gram-positive bacteria (*S. aureus* (MTCC 3381), *B. cereus* (MTCC 0430)). The microbial results are given in Table 4. The newly synthesized ligands ( $\text{L}^1\text{H}$  &  $\text{L}^2\text{H}$ ) and their silicon complexes showed zone of inhibition ranging 10.7–22.6 mm against *S. aureus*, 8.8–19.8 mm against *B. cereus*, 8.6–24.5 mm against *E. coli* and 9.7–22.3 mm against *K. pneumoniae*. In the whole series, MIC of synthesized compounds ranged between, 200 and 0.39  $\mu\text{g}/\text{mL}$  against all microorganisms. Compound  $\text{Me}_3\text{SiL}^1$  were found to be best as they exhibited the lowest MIC of 1.56  $\mu\text{g}/\text{mL}$  against *E. coli* and 3.125  $\mu\text{g}/\text{mL}$  against *Klebsiella sp.* (Table 5). The other compound  $\text{PhSi}(\text{L}^3)\text{OEt}$  also exhibited good MIC value i.e. 6.25  $\mu\text{g}/\text{mL}$  against *S. aureus*, *B. cereus*.  $\text{Me}_3\text{SiL}^1$  is found to show maximum activity against *E. coli* with zone of inhibition 24.5 mm, i.e. near to standard drugs. However other tested compounds showed moderate antibacterial activity. It has been observed that the metal complexes showed an increased zone of inhibition against the bacterial strains as compared to ligands. A marked enhancement of in vitro biocidal studies of ligands was exhibited in coordination with silicon atom against all microorganisms' strains under tested identical experimental conditions.

The biological activity of the Schiff base exhibited a considerable enhancement on coordination with the metal ion against all bacterial strains. This enhancement in the activity may be rationalized on the basis that its structure mainly possess an additional  $>\text{C}=\text{N}$  bond. It has been suggested that Schiff base with nitrogen and sulfur/oxygen donor systems inhibit enzyme activity, since the enzymes which require these groups for their activity appear to be especially more susceptible to deactivation by metal ions on coordination. Moreover, coordination reduces the polarity of the metal ion mainly because of the partial sharing of its positive charge with the donor groups (Meyer et al., 1982; Chohan et al., 2002) within the chelate ring system formed during coordination Singh et al., 2013a,b,c).

**Table 4** Antibacterial activity of thiosemicarbazone and semicarbazone and their complexes.

Compounds	Inhibition zone (mm)			
	<i>E. coli</i>	<i>K. pneumoniae</i>	<i>B. cereus</i>	<i>S. aureus</i>
L <sup>1</sup> H	15.2	18.1	10.7	8.8
Me <sub>3</sub> SiL <sup>1</sup>	24.5	21.6	22.6	17.2
PhSi(L <sup>1</sup> )OEt	18.6	22.3	18.2	19.8
L <sup>3</sup> H	8.6	9.7	12.5	14.6
Me <sub>3</sub> SiL <sup>3</sup>	14.8	18.5	13.1	11.4
PhSi(L <sup>3</sup> )OEt	16.8	18.6	18.2	19.8
Streptomycin	24.4	25.2	22.7	20.6
Ciprofloxacin	25.1	26.0	24.2	26.5
DMSO	0	0	0	0

**Table 5** Minimum inhibitory concentration (MIC) (μg/ml) of the ligands and their organosilicon(IV) complexes.

Compounds	Bacteria			
	<i>E. coli</i>	<i>K. pneumoniae</i>	<i>B. cereus</i>	<i>S. aureus</i>
L <sup>1</sup> H	25.0	25.0	50.0	50.0
Me <sub>3</sub> SiL <sup>1</sup>	1.5625	3.125	6.25	12.5
PhSi(L <sup>1</sup> )OEt	6.25	6.25	12.5	12.5
L <sup>3</sup> H	25.0	25.0	25.0	25.0
Me <sub>3</sub> SiL <sup>3</sup>	12.5	6.25	12.5	6.25
PhSi(L <sup>3</sup> )OEt	12.5	6.25	6.25	6.25
Streptomycin	1.5625	3.125	3.125	3.125
Ciprofloxacin	3.125	3.125	6.25	6.25

This process, in turn, increases the lipophilic nature of the central metal atom (Singh et al., 2014), which favors its penetration of the metal complexes into the lipid layer of cell membrane resulting in interference with normal cell process and also disturbing the respiration process of cell and blocking the synthesis of proteins, which further restricts growth of organisms. Some important factors such as the nature of the metal ion, nature of the ligand, coordinating sites, and geometry of complex, concentration, lipophilicity and presence of co-ligands have a considerable influence on antibacterial activity. Certainly, steric and pharmacokinetic factors also play a decisive role in deciding the potency of an antimicrobial agent. The presence of lipophilic and polar substituent is expected to enhance antibacterial activity. Thus antibacterial property of metal complexes cannot be ascribed to chelation alone, but it is a complicated mix of several contributions. Thus it can be postulated that further studies of these complexes in this direction could lead to more interesting results.

#### 4. Conclusion

We report here the synthesis and characterization of new complexes of organosilicon(IV) with sulfur, oxygen and nitrogen donor ligands. The ligand coordinates to the organosilicon(IV) ions through the phenolic oxygen, azomethine nitrogen and sulfur/oxygen atoms. Based on the spectral and DFT calculations, trigonal bipyramidal and distorted octahedral structures have been assigned to all the complexes. The antibacterial activity screening of the silicon complexes showed varied activities but they are more active than the free ligands. The MIC determinations revealed that the Me<sub>3</sub>SiL<sup>1</sup> complexes are more active.

#### Conflict of interest

The authors have declared no conflict of interest.

#### Acknowledgments

The authors are thankful to Dean, CET, and Dean, CASH, Mody University of Science and Technology, Laxmangarh, Sikar, for providing necessary facilities to carry out this research work.

#### Appendix A. Supplementary data

Supplementary data associated with this article can be found, in the online version, at <http://dx.doi.org/10.1016/j.jaubas.2016.05.003>.

#### References

- Al-Burtamani, S.K.S., Fatope, M.O., Marwah, R.G., Onifade, A.K., Al-Saidi, S.H., 2005. Chemical composition, antibacterial and antifungal activities of the essential oil of *Haplophyllum tuberculatum* from Oman. *J. Ethnopharmacol.* 96, 107–112.
- Ali, M.R., Marella, A., Alam, M.T., Naz, R., Akhter, M., Shaquiquz-zaman, M., Saha, R., Tanwar, O., Alam, M.M., Hooda, J., 2012. Review of biological activities of hydrazones. *Indonesian J. Pharm.* 23 (3), 193–202.
- Arora, S., Agarwal, S., Singhal, S., 2014. Anticancer activities of thiosemicarbazides/thiosemicarbazones: a review. *Int. J. Pharm. Pharm. Sci.* 6 (9), 34–41.
- Asif, M., Husain, A., 2013. Analgesic, anti-inflammatory and antiplatelet profile of hydrazones containing synthetic molecules. *J. Appl. Chem.*, <http://dxdoi.org/10.1155/2013/247203>.
- Becke, A.D., 1986. Density functional calculations of molecular bond energies. *J. Chem. Phys.* 84, 4524–4529.
- Chohan, Z.H., Scozzafava, A., Supran, C.T., 2002. Unsymmetrical 1,1'-disubstituted Ferrocenes: synthesis of Co(ii), Cu(ii), Ni(ii) and Zn(ii) chelates of Ferrocenyl -1-thiadiazolo-1'-tetrazole, -1-thiadiazolo-1'-triazole and -1-tetrazolo-1'-triazole with Antimicrobial Properties. *J. Enzyme Inhib. Med. Chem.* 17, 261–266.
- Chuit, C., Corriu, R.J.P., Reye, C., In, K.-Y., 1999. In: Akiba (Ed.), *Chemistry of Hypervalent Compounds*. Wiley-VCH, New York, pp. 81–146.
- Devi, J., Kumari, S., Asijaa, S., Malhotra, R., 2012. Synthetic, spectroscopic, and biological aspects of triorganosilicon(IV) complexes of tridentate Schiff bases. *Phosphorus, Sulfur, and Silicon and the Related Elements* vol. 187, 1409–1417.
- Frisch, M.J., Trucks, G.W., Schlegel, H.B., Scuseria, G.E., Robb, M.A., Cheeseman, J.R., Montgomery, J.A., Vreven, T., Kudin, K.N., Burant, J.C., Millam, J.M., Iyengar, S.S., Tomasi, J., Barone, V., Mennucci, B., Cossi, M., Scalmani, G., Rega, N., Petersson, G.A., Nakatsuji, H., Hada, M., Ehara, M., Toyota, K., Fukuda, R., Hasegawa, J., Ishida, M., Nakajima, T., Honda, Y., Kitao, O., Nakai, H., Klene, M., Li, X., Knox, J.E., Hratchian, H.P., Cross, J.B., Adamo, C., Jaramillo, J., Gomperts, R., Stratmann, R.E., Yazyev, O., Austin, A.J., Cammi, R., Pomelli, C., Ochterski, J.W., Ayala, P. Y., Morokuma, K., Voth, G.A., Salvador, P., Dannenberg, J.J., Zakrzewski, V.G., Dapprich, S., Daniels, A.D., Strain, M.C., Farkas, O., Malick, D.K., Rabuck, A.D., Raghavachari, K., Foresman, J.B., Ortiz, J.V., Cui, Q., Baboul, A.G., Clifford, S., Cioslowski, J., Stefanov, B.B., Liu, G., Liashenko, A., Piskorz, P., Komaromi, I., Martin, R.L., Fox, D.J., Keith, T., Al-Laham, M.A., Peng, C.Y., Nanayakkara, A., Challacombe, M., Gill, P.M.W., Johnson, B., Chen, W., Wong, M.W., Gonzalez, C., Pople, J.A., 2004. GAUSSIAN 03, Revision C.01. Gaussian Inc., Wallingford, CT.
- González-García, G., Álvarez, E., Marcos-Fernández, A., Gutiérrez, J. A., 2009. Hexa-coordinated oligosilanes from a hexa-coordinated



- silicon(IV) complex containing an O, N, N, O salen-type and thiocyanato-N ligands. *Inorg. Chem.* 48 (9), 4231–4238.
- Kadish, K.M., Xu, Q.Y., Barbe, J.M., Guillard, R., 1988. Synthesis and reactivity of sigma-bonded silicon metalloporphyrins: Spectroscopic characterization and electrochemistry of (P)Si(R)<sub>2</sub>, (P)Si(R)X, and (P)SiX<sub>2</sub>, where R = C<sub>6</sub>H<sub>5</sub> or CH<sub>3</sub> and X = OH<sup>-</sup> or ClO<sub>4</sub><sup>-</sup>. *Inorg. Chem.* 27 (7), 1191–1198.
- Kalaivani, P., Prabhakaran, R., Dallemer, F., Poornima, P., Vaishnavi, E., Ramachandran, E., Padma, V.V., Renganathan, R., Natarajan, K., 2012. DNA, protein binding, cytotoxicity, cellular uptake and antibacterial activities of new palladium(II) complexes of thiosemicarbazone ligands: effects of substitution on biological activity. *Metallomics* 4, 101–113.
- Kothari, R., Sharma, B., 2014. Synthesis, characterization, antibacterial, antifungal, antioxidant and dna interaction studies of thiosemicarbazone transition metal complexes. *World J. Pharm. Pharm. Sci.* 3 (7), 1067–1080.
- Kulandaivelu, U., Padmini, V.G., Suneetha, K., Shireesha, B., Vidyasagar, J.V., Rao, T.R., Jayaveera, K.N., Basu, A., Jayaprakash, V., 2011. Synthesis, antimicrobial and anticancer activity of new thiosemicarbazone derivatives. *Arch. Pharm.* 344 (2), 84–90.
- Kumar, S., Raj, V., 2013. Review on anticonvulsant activity of semicarbazones. *Inter. J. Phytotherapy* 3 (2), 37–46.
- Malhotra, R., Mehta, J., Puri, J.K., 2007. Heterobimetallic complexes containing iron(II) and hexa-coordinated organosilicon. *Central Eur. J. Chem.* 5 (3), 858–867.
- Meyer, B.N., Ferrigni, N.R., Putnam, J.E., Jacobsen, L.B., Nichols, D. E., McLauhglin, J.L., 1982. Brine shrimp: a convenient general bioassay for active plant constituents. *Planta Med.* 45, 31–34.
- Mohamed, G.G., Omar, M.M., Hindy, A.M., 2006. Metal complexes of Schiff bases: preparation, characterization, and biological activity. *Turk. J. Chem.* 30 (3), 361–382.
- Mohamed, N.A., Mohamed, R.R., Seoudi, R.S., 2014. Synthesis and characterization of some novel antimicrobial thiosemicarbazone *o*-carboxymethyl chitosan derivatives. *Int. J. Biol. Macromol.* 63, 163–169.
- Naidu, P.V.S., Kinthada, P.M.M.S., 2012. Structure and biological activities of novel phytochemicals Cu(II)-quercetin thiosemicarbazone and its derivatives: potential anti-cancer drugs. *Int. J. Pharm. Med. & Bio. Sci.* 1 (2), 55–65.
- Nath, M., Goyal, S., Goyal, S., 2000. Synthesis, spectral and biological studies of organosilicon(IV) complexes of Schiff bases derived from amino acids. *Synth. React. Inorg. Met.-Org. Chem.* 30 (9), 1791–1804.
- Pahontu, E., Julea, F., Rosu, T., Purcarea, V., Chumakov, Y., Petrenco, P., Gulea, A., 2015. Antibacterial, antifungal and *in vitro* antileukaemia activity of metal complexes with thiosemicarbazones. *J. Cell Mol. Med.* 19 (4), 865–878.
- Reis, D.C., Despaigne, A.A.R., Da Silva, J.G., Silva, N.F., Vilela, C. F., Mendes, I.C., Takahashi, J.A., Beraldo, H., 2013. Structural studies and investigation on the activity of imidazole-derived thiosemicarbazones and hydrazones against crop-related fungi. *Molecules* 18 (10), 12645–12662.
- Savithiri, S., Doss, M.A., Rajarajan, G., Thanikachalam, V., 2014. Synthesis, spectral, stereochemical and antimicrobial evaluation of some 3*t*-pentyl-2*r*,6*c*-diarylpiperidin-4-one thiosemicarbazone derivatives. *Can. Chem. Trans.* 2 (4), 403–417.
- Sedaghat, T., Pour, Z.S., 2009. Synthesis and spectroscopic studies of new organotin(IV) complexes with tridentate N- and O-donor Schiff bases. *J. Coord. Chem.* 62 (23), 3837–3844.
- Seiler, O., Burschka, C., Fenske, T., Troegel, D., Tacke, R., 2007. Neutral hexa- and pentacoordinate silicon(IV) complexes with SiO<sub>6</sub> and SiO<sub>4</sub>N skeletons. *Inorg. Chem.* 46 (13), 5419–5424.
- Sidir, I., Sidir, Y.G., Kumalar, M., Taşal, E., 2010. Ab initio Hartree-Fock and density functional theory investigations on the conformational stability, molecular structure and vibrational spectra of 7-acetoxy-6-(2,3-dibromopropyl)-4,8-dimethylcoumarin molecule. *J. Mol. Struct.* 964 (1–3), 134–151.
- Silva, M.J., Alves, A.J., Nascimento, S.C.D., 1998. Synthesis and cytotoxic activity of *N*-substituted thiosemicarbazones of 3-(3,4-methylenedioxy)phenylpropanal. *II Farmaco* 53 (3), 241–243.
- Singh, H.L., 2009. Synthesis, spectral, and 3D molecular modeling of tin(II) and organotin(IV) complexes of biologically active Schiff bases having nitrogen and sulfur donor ligands. *Phosphorus, Sulfur Silicon* 184, 1768–1778.
- Singh, M.S., Singh, P.K., 2000. A new class of organosilicon(IV) compounds based upon tetradentate (N<sub>2</sub>O<sub>2</sub>) chelating ligand. *Main Group Metal Chem.* 23 (3), 183–188.
- Singh, H.L., Khungar, B., Tripaathi, U.D., Varshney, A.K., 2001. Spectral and antimicrobial studies of organotin(IV) complexes of bidentate schiff bases having nitrogen and sulphur donor systems. *Main Group Metal Chem.* 24, 5–12.
- Singh, H.L., Singh, J.B., Sharma, K.P., 2012. Synthetic, structural, and antimicrobial studies of organotin(IV) complexes of semicarbazone, thiosemicarbazone derived from 4-hydroxy-3- methoxy-benzaldehyde. *Res. Chem. Intermed.* 38, 53–65.
- Singh, H.L., Singh, J., Mukherjee, A., 2013a. Synthesis, spectral, and *in vitro* antibacterial studies of organosilicon(IV) complexes with Schiff bases derived from amino acids. *Bioinorg. Chem. Appl.*, <http://dxdoi.org/10.1155/2013/425832>.
- Singh, H.L., Singh, J.B., Sachedva, H., 2013b. Synthesis, spectroscopic and antimicrobial studies of lead(II) complexes of Schiff bases derived from amino acids and isatins. *Spectrosc. Lett.* 46, 286–296.
- Singh, K., Puri, P., Kumar, Y., Sharma, C., 2013c. Organosilicon(IV) and organotin(IV) complexes of biologically potent 1,2,4- triazole derived Schiff bases: Syntheses, spectral studies and *in vitro* antimicrobial activity. *Int. J. Inorg. Bioinorganic Chem.* 3 (4), 57–64.
- Singh, H.L., Singh, J., Chauhan, S.S., Mukherjee, A., Dewa, T., 2014. Synthetic, structural, theoretical and biological study of triorganotin(IV) Schiff base complexes derived from amino acids. *J. Chem. Pharm. Res.* 6 (11), 248–257.
- Singh, H.L., Singh, J.B., Bhaunka, S., 2015. Synthesis, spectroscopic characterization, biological screening, and theoretical studies of organotin(IV) complexes of semicarbazone and thiosemicarbazones derived from (2-hydroxyphenyl)(pyrrolidin-1-yl)methanone. *Res. Chem. Intermed.*, <http://dxdoi.org/10.1007/s11164-015-2069-3>.
- Singh, H.L., Singh, J.B., Bhaunka, S., 2016. Synthesis, spectral, DFT, and antimicrobial studies of tin(II) and lead(II) complexes with semicarbazone and thiosemicarbazones derived from (2-hydroxyphenyl)(pyrrolidin-1-yl)methanone. *J. Coord. Chem.* 69, 343–353.
- Singhal, M., Paul, A., Singh, H.P., Dubey, S.K., Songara, P.K., 2011. Synthesis and evaluation of antioxidant activity of semicarbazone derivatives. *Inter. J. Pharma. Sci. Drug Res.* 3 (2), 150–154.
- Tang, G.-D., Zhao, J.-Y., Li, R.-Q., Yuan-Cao, Zhang, Z.-C., 2011. Synthesis, characteristic and theoretical investigation of the structure, electronic properties and second-order nonlinearity of salicylaldehyde Schiff base and their derivatives. *Spectrochim. Acta, Part A* 78 (1), 449–457.
- Thanh, N.D., Duc, H.T., Duyen, V.H., Tuong, P.M., Quoc, N.V., 2015. Synthesis, antibacterial and antifungal activities of N-(tetra-O-acetyl-β-D-glucopyranosyl) thiosemicarbazones of substituted 4-formylsydnones. *Chem. Cent. J.* <http://dx.doi.org/10.1186/s13065-015-0138-8>.
- Tojal, J.G., 2012. Thiosemicarbazones as new antitumor compounds. *Electron J. Biomed.* 1, 11–15.
- Varshney, A.K., Varshney, S., Sharma, M., Singh, H.L., 2000. Synthetic, spectral and biological studies of organosilicon(IV) complexes with Schiff bases of sulfa drugs. *Phosphorus, Sulfur Silicon Relat. Elem.* 161, 163–172.
- Wang, Q., Ding, R., Wen, X., Yin, F., 2013. Synthesis, characterization, and structure of some silicon containing diorganotin(IV) complexes of salicylaldehyde thiosemicarbazones. *Phosphorus, Sulfur Silicon Relat. Elem.* 188 (7), 895–903.